10th International Conference on Composite Science and Technology
ICCST/10
A.L. Araújo, J.R. Correia, C.M. Mota Soares, et al. (Editors)

EFFECT OF REACTIVE RUBBER NANOPARTICLES AND NANOCLAY MIX ON THE MECHANICAL PROPERTIES OF EPOXY

Mona A. Ahmed[†], Usama F. Kandil[*], Neviene O. Shaker[††], Ahmed I. Hashem[**]

[†]Graduate Research Assistant
Polymer Nanocomposites Center, Egyptian Petroleum Research Institute, Egypt
mona_chemist17@yahoo.com

[*]Associate Professor
Polymer Nanocomposites Center, Egyptian Petroleum Research Institute, Egypt
alfa_olefins@yahoo.com

[††]Professor
Polymer Nanocomposites Center, Egyptian Petroleum Research Institute, Egypt
shaker_no@yahoo.com

[**]Professor
Department of Chemistry, Ain Shams University, Egypt
ahmed_hashem@sci.asu.edu.eg

Keywords: Reactive Rubber Nanoparticles, Toughness, Stiffness and Nanocomposites

Summary: *While epoxy is the most used adhesive in structural applications, it suffers from brittle behavior at failure and relatively low energy absorption (toughness). The main objective of this work is to examine the effect of incorporating a mix of reactive rubber nanoparticles (RRNP) and organically modified nanoclay (Cloisite-30B) into the epoxy matrix with the aim of improving material toughness without compromising its desired strength and stiffness. Epoxy (amine based) hybrid nanocomposites containing RRNP, Cloisite-30B and a mix of RRNP/Cloisite-30B were synthesized and mechanically characterized. Mechanical characterization was performed using the nanoindentation technique to extract the elastic modulus and toughness of the material. 10 μm Spherical indention tip was used to probe the surface of the epoxy nanocomposites. Microstructural characterization using X-ray diffraction (XRD) and transmission electron microscopy (TEM) was performed to investigate the significance of nanoclay exfoliation on the mechanical properties. Furthermore, Incorporation of RRNP results in softening the epoxy nanocomposite and lowering its stiffness and thus improving its toughness compared with neat epoxy. In contrast, incorporation of Cloisite-30B increased the stiffness and lowered the toughness of the epoxy/nanocomposites compared with neat epoxy. The balance between RRNP and Cloisite-30B led to hybrid nanocomposites with improved energy absorption and acceptable stiffness for structural applications.*

1. INRTODUCTION

Epoxy resins are an important class of polymeric materials for their excellent strength and stiffness, impressive chemical, thermal, and dimensional stability, good creep and solvent resistance, and strong adhesion to metal and ceramic surfaces [1]. These superior performances characteristics, together with their formulation versatility, excellent

processability, and reasonable cost, have made epoxy resins attractive for a wide variety of engineering applications [1]. So, toughening of brittle epoxy thermosets has been intensively studied in the past few decades since the lack of toughness is one of the major reasons limiting their more widespread engineering applications [2,3]. One of the most successful strategies of improving the fracture toughness of epoxy is to introduce a second phase into the epoxy matrix. In these systems, the fracture toughness can be increased by forming multiphase morphology with the ability to initiate various toughening mechanisms during crack growth [4, 5, 6].

Since the pioneering advances of *B.F. Goodrich* researchers during the 1970s, the incorporation of liquid rubbers is used extensively to improve toughness/stiffness balance of thermosets[7]. Several requirements must be met in the development of toughening agents: solubility in the uncured resin without massive increase of solution viscosity and phase separation during cure. The compatibility between liquid rubber and resin must be matched carefully in order to achieve phase separation during cure and simultaneously provide adequate interfacial adhesion [8]. The phase-separated rubber particles are presumed to act as stress concentrators initiating energy absorbing "toughening" processes. According to the literature, the most common micromechanical processes responsible for the increase in fracture toughness are localized shear yielding of the epoxy matrix, plastic void growth in the matrix, which is initiated by cavitation or deboning of the rubber particles, and rubber particle bridging behind the crack tip [9,10].

Nanocomposite technology using organophilic layered silicates as an *in-situ* route to nano-reinforcement offers new opportunities for the modification of thermoset micromechanics. Large improvements of mechanical and physical properties including modulus [11], barrier properties [12], flammability resistance [13], and ablation performance [14] have been reported for this type of material at low silicate content. In principle, it should be possible to compensate matrix flexibilization via matrix reinforcement using organophilic layered silicates.

Therefore, the main objective of this work is to incorporate both reactive rubber nanoparticles (RRNP) and organically modified nanoclay (Cloisite- 30B) into epoxy matrix with the aim of obtaining improved material with toughness higher than neat epoxy, epoxy/clay and epoxy/RRNP hybrids without compromising the other desired mechanical properties. Epoxy hybrid nanocomposites containing both fillers; organo-modified montmorillonite (o-mmt) and reactive rubber nanoparticles (RRNP); were synthesized in order to combine their enhancing properties which normally result from the use of the single fillers and hence aiming to improve toughness/stiffness balance. Although the fracture and deformation behavior of the epoxy-nanocomposites have been intensively studied at the macro-level over the past decade, less attention has been paid to the stress transfer mechanism in the nano to micro-level behavior of nanoclay and nanorubber interactions with epoxy.

2. METHODS

2.1. Materials and Procedure

Oleic acid (Adwic co) as a surfactant, potassium hydroxide (TOK co), toluene (fision, AR), chloroform (Aldrich ,99.8%) are all of analytical grade and were used as received. Deionized water was used for all latices. Divinylbenzene (Merch, inhibited by 4-tertbutyl catechol) as a crosslinker was washed over 10wt% NaOH solution. Styrene-co-butadiene rubber (SBR-latex) (Sika Co.), benzoyl peroxide (BPO) (moistened with 25% water, Loba Chemie), ammonium persulphate (Morgan, 98%), and HCL (37%, Aldrich CO), methanol (95%,

Aldrich CO) were used as received. The resin is a low viscosity 100% reactive diluted liquid based on bisphenol-A containing EPOTUF®37-058 which is C_{12}–C_{14} glycidyl ether, while the hardener is Aliphatic Amine EPOTUF®37-614. The clay used to synthesize epoxy–clay nanocomposite is Cloisites30B supplied by Southern Clay Products, Inc. The rubber nanoparticles were first dispersed in chloroform before mixing with the epoxy base resin using ultrasonicator. This was followed by evaporation of chloroform and adding the epoxy hardener; then casting in molds for flexural testing. According to ASTM D790-98; five rubber nanoparticle contents were examined including 0, 3, 5, 7 and 10 wt% of resin.

2.2. Fabrication of clay nanoparticles/epoxy nanocomposite

Five nanoclay contents were examined including 2, 4, 6, 8 and 10wt% of resin. Relatively, high operating temperature and ultrasonication facilitate diffusion of oligomers inside the clay galleries. The nanoclay was dispersed in the epoxy resin at 120^{o}C using a mechanical stirrer at about 1200 rpm for 2 hours followed by further dispersion with an ultrasonic probe for 2 hours at 60^{o}C (**Figure 1**). While mixing, the beaker was placed in a cold water bath to avoid temperature increase of the dispersion during the sonication process and the temperature was monitored [15]. Then, the dispersion was cooled to room temperature followed by adding the hardener, stirred for about two more minutes. The epoxy–clay nanocomposite was then casted in molds and left to cure at room temperature for 14 days for flexural testing (**Figure 1**).

Figure 1: (a) Dispersion of Cloisite- 30B in the epoxy using ultrasonic processor; (b) Nanoclay modified epoxy: sample preparation and casting for flexural testing.

2.3. Mechanical Testing

Flexural testing was used to characterize flexural strength and stiffness of epoxy nanocomposites to verify consistency in samples. Dynamic mechanical analyzer (DMA) supplied from Triton Technology (TTDMA), U.K., was used to study the viscoelastic properties of the nanocomposites as a function of clay concentration and then correlated with the morphology.

2.4. Microstructrual Investigation

Chemical bonds of epoxidized rubber particles were investigated by Fourier transform infrared spectroscopy (FTIR), H^{1}NMR, Bulk morphology in the polymer films was examined by Scanning Electron Microscope (SEM),(TEM). In addition, to explain the effect of nanoclay on the behavior of epoxy–clay nanocomposite, the degree of clay intercalation and exfoliation was investigated using X-ray diffraction (XRD).

3. RESULTS AND DISCUSSION

3.1. Microstructrual Characterization

The epoxy functional group located on the surface of rubber nanoparticles enhances the reactivity of these particles during the curing reaction of epoxy. This can be observed from **Figure 2** which shows the SEM micrographs of the fracture surface of a simple blend

between unfunctionalized rubber nanoparticles and epoxy resin (**Figure 2-left**) with epoxidized particles/epoxy reactive blend (**Figure 2-right**). In case of a simple blend, there are a lot of concave holes and convex particles in its fracture surface which indicates the weakness of adhesion between the rubber nanoparticles and the epoxy matrix. On the other hand, this view disappeared in the reactive blend between epoxidized nanoparticles with the epoxy matrix. This is attributed to the incorporation of the surface epoxy groups of the particles during the epoxy curing reaction. This reaction enhances the adhesive force between the epoxy matrix and the particles and exceeds the matrix cohesive force (**Figure 2-right**). In addition, the cross-linked rubber nanoparticles are uniformly distributed in the epoxy matrix as shown in the TEM micrograph of the epoxy/RRNP reactive blend (**Figure 3**). This is an essential requirement for toughening mechanism. Consequently, the resulting core-shell reactive rubber nanoparticles (RRNP) are homogeneously embedded in the epoxy matrix with interfacial interactions.

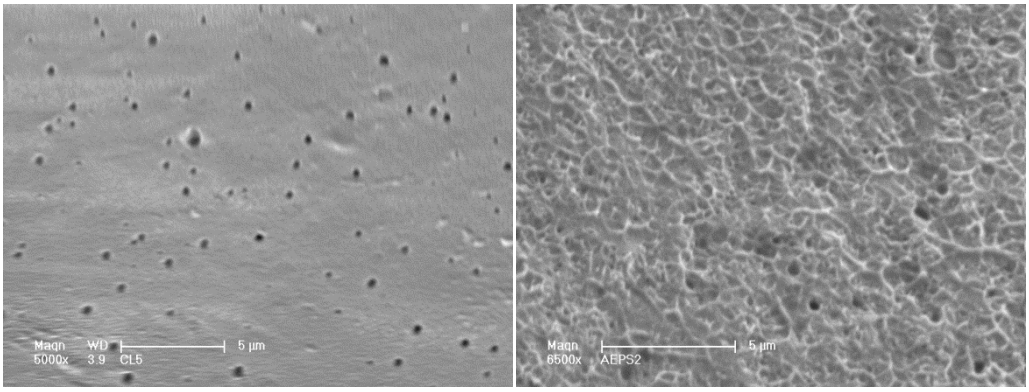

Figure 2: SEM micrographs of a simple blend between un-functionalized rubber nanoparticles and epoxy resin (left); and reactive blend between epoxidized particles and epoxy resin (right).

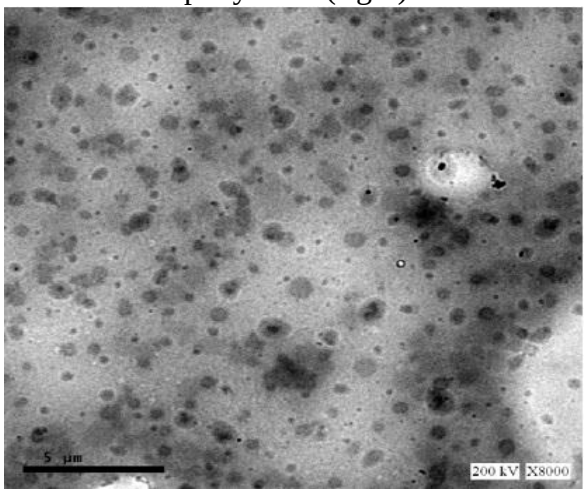

Figure 3: TEM micrograph of epoxy toughened with 5% **RRNP**

Figure 4 shows the ^{1}H NMR spectra of (a) SBR and (b) epoxidized SBR rubber nanoparticles. The ^{1}H-NMR spectrum of SBR (Fig. 10a) shows a peak at δ = 5.4 ppm that is attributed to *trans*- and *cis*-1,4 hydrogens and a peak at δ = 4.9 ppm for two terminally vinylic hydrogens. Aromatic hydrogen peaks and the peak of the styrenic hydrogen of the styrene unit appear at δ = 7.2 ppm and δ = 2.5 ppm, respectively. The ^{1}H-NMR spectrum of epoxidized SBR (Fig. 5b) shows new peaks at δ = 2.5–2.7 and δ = 3.1 ppm corresponding to the methylene resonance of the epoxy groups in the *trans*-, vinyl- and *cis*-position, respectively [16]. By comparing (a) and (b) spectra, it is clear that the vinylic protons were

completely disappeared on epoxidizing with *m*-chloroperbenzoic acid and the appearance of two new peaks attributed to the epoxy ring protons.

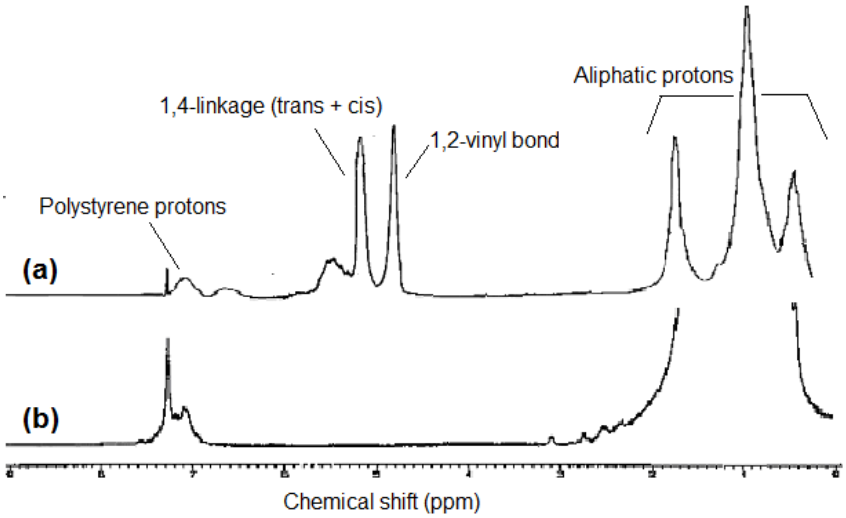

Figure 4: ^{1}H NMR (a) SBR, and (b) epoxidized rubber nanoparticles.

The FT-IR spectra of SBR and epoxidized SBR are shown in **Figure 5(a&b)**, respectively. By comparing both spectra, it is clear that (Fig. 6a) showed a band at 699 cm^{-1} that is related to 1,4-*cis*, a band at 910 cm^{-1} to 1,2-vinyl double bonds, and a band at 969 cm^{-1} to 1,4-*trans*, respectively. In the FT-IR spectrum of epoxidized SBR (Fig. 6b) the bonds of stretching and contracting in phase of all epoxy rings were observed at about 1258 and 842 cm^{-1} [16].

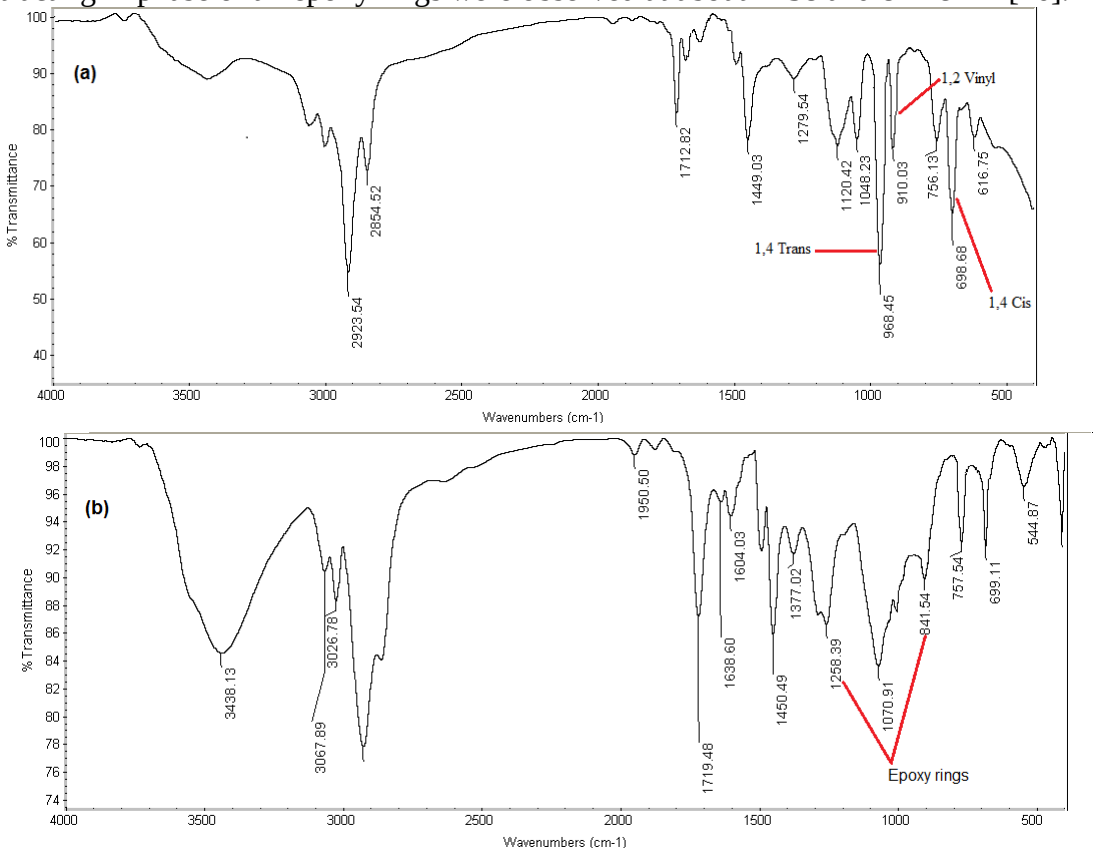

Figure 5: a) FTIR of SBR , b) epoxidized SBR nanoparticles

Figure 6 shows the XRD of patterns of epoxy–clay nanocomposites. Table 1 shows XRD values for Cloisite 30B and its epoxy nanocomposites containing 2, 4, 6, 8, and 10 wt. % clay

contents**.** Using Eq. (1), $\lambda=2d\sin\theta$ *(Bragg's law)*, the characteristic (001) of nanoclay appeared at 2θ=4.62°, therefore the d-spacing of nanoclay was determined to be 1.91 nm. The (001) peaks of all wt% of nanoclay epoxy–clay nanocomposites appeared in the range of 2θ=2.1° to 2θ=2.3° indicating the presence of intercalations with d-spacing of 4.20 nm to 3.83 nm, respectively and almost disappearance of the nanoclay main peak. This is an evidence of complete dispersion of the nanoclay in the epoxy matrix. In addition, by comparing the relative intensities for all nanoclay percentages, it could be concluded that nanoclay dispersion might be in both intercalation and exfoliation modes depending on the nanoclay percentage for each.

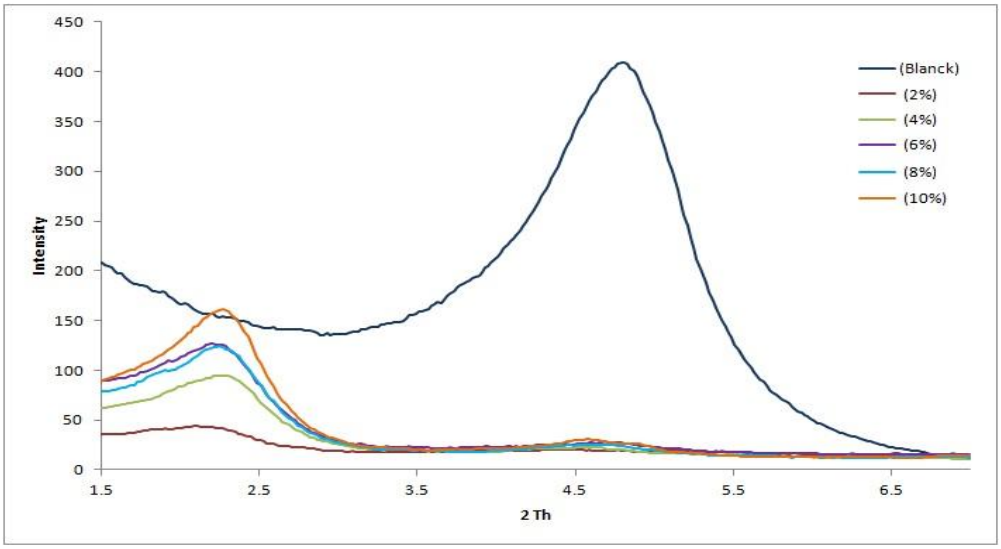

Figure 6: X-ray diffraction patterns of Cloisite 30B and epoxy/ Cloisite 30B nanocomposites containing 2, 4, 6, 8, and 10 wt. % clay contents**.**

Table 1: XRD values for Cloisite 30B and its epoxy nanocomposites containing 2, 4, 6, 8, and 10 wt. % clay contents**.**

Sample	$2\theta^{o}$	d-spacing
2 wt%	2.10	4.20
4 wt%	2.20	4.01
6 wt%	2.20	4.01
8 wt%	2.23	3.95
10 wt%	2.30	3.83
Cloisite 30B	4.62	1.91

3.3. Mechanical Characterization

Flexural stress-strain curves of epoxy/clay, epoxy/RRNP and epoxy/clay/RRNP nanocomposites are given in **Figures 7, 8, 9**; respectively. It is appeared that the incorporation of nanoclay into epoxy matrix improved its flexural modulus as shown in **Figure 7.** The improved modulus can be directly ascribed to the stiffening effect of clay fillers since the clay has a higher modulus than epoxy. The diminishing improvement in flexural modulus at high clay (8%, 10%) contents is attributed to the higher possibility of forming unwanted agglomerates, which in turn reduced the reinforcing efficiency of clay. **Figure 8** represents flexural properties of the cured epoxy samples containing different amount of the RRNP. All the modified epoxy networks exhibit higher strain at failure than non-modified epoxy while significantly reducing its stiffness and ultimate strength. The reduction in strength is attributed to the presence of rubber, which is distributed in the epoxy.

Based on **Figure 8**; it is evident that the best performance was normally achieved with 5 wt% of RRNP which give higher strain than neat epoxy with less stiffness so the higher toughness (area under the curve) than all epoxy/RRNP contents.

Finally, in the present work; the optimal percentages of nanoclay and RRNP have been incorporated into the epoxy matrix for obtaining the best hybrid flexural properties. **Figure 9** represents typical flexural stress-strain curves of pristine resin and different modified epoxies. All curves show apparent ductility with different modulus, ultimate strength, and fracture strain. The pristine resin has high yield strength but the lowest fracture strain. It is clear from the figure that the incorporation of 5 wt% RRNP into epoxy matrix increases fracture strain. However, this was accompanied by reduction in yield strength, modulus and ultimate strength. On the other hand; the incorporation of 6 wt% nanoclay into epoxy matrix increases fracture stress with some reduction in the strain value. Consequently; combining these two optimal percentages of RRNP and nanoclay into the epoxy matrix enhanced the flexural stress-strain curve as shown in the formed hybrid.

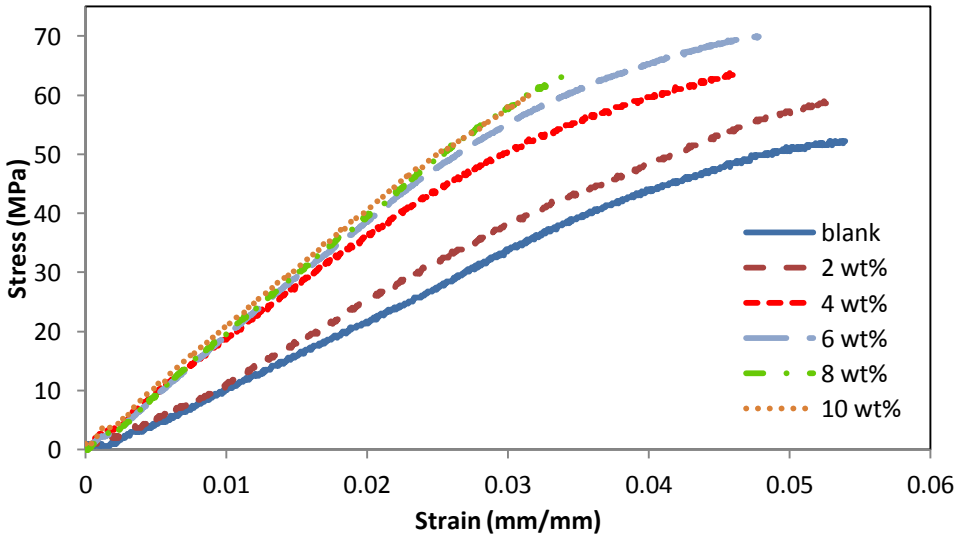

Figure 7: Typical flexural stress-strain curves of pristine resin and nanoclay modified epoxy

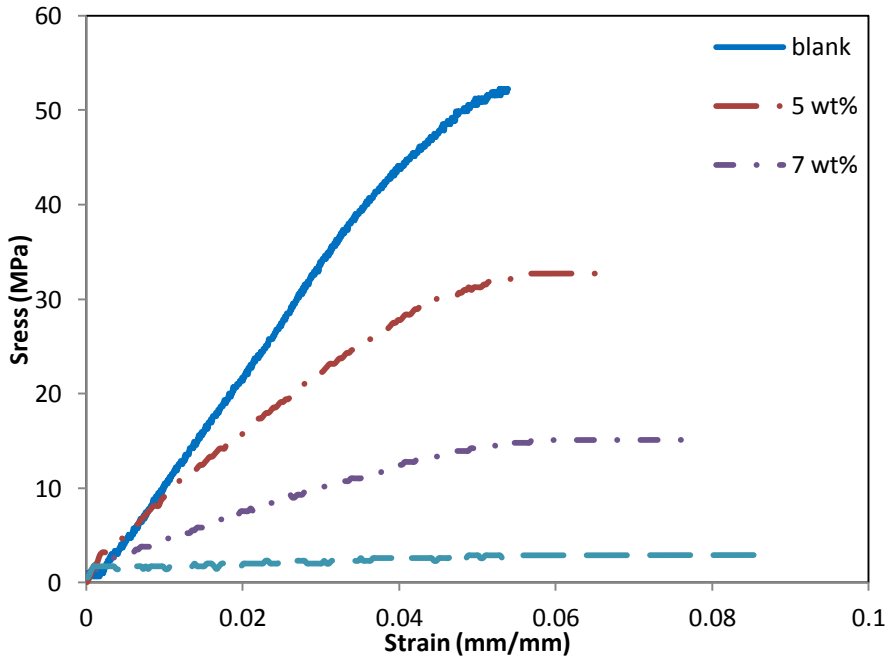

Figure 8: Typical flexural stress-strain curves of pristine resin and RRNP modified epoxy

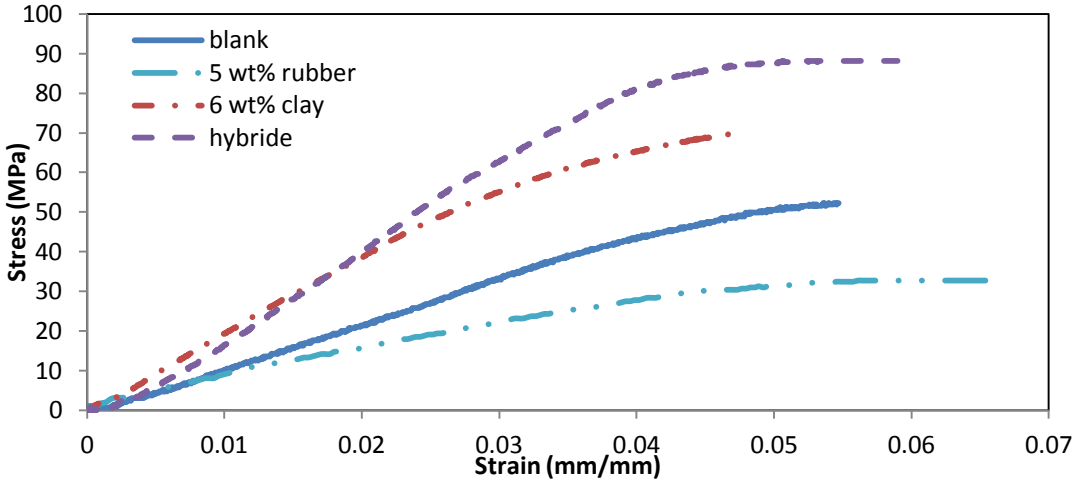

Figure 9: Typical flexural stress-strain curves of pristine resin and modified epoxies

Dynamic mechanical properties (DMA):

Table 2 shows the storage modulus (E) values versus crosslink density (M_c) for clay/epoxy, RRNP/epoxy and clay/RRNP/epoxy nanocomposites at ambient temperature.

Table 3: Values of storage modulus (E) vs. crosslink density (M_c) in clay/epoxy, RRNP/epoxy and clay/RRNP/epoxy nanocomposites at ambient temperature.

Clay (wt%)	*Rubber (wt%)*	*Storage modulus* G_r (Pa)*	*Density (mg/cm^3)*	*M_c (mg/mole)*
0	0	9.05E+06	0.45	0.124
4	0	1.91E+07	0.94	0.119
6	0	5.27E+07	1.11	0.0513
8	0	4.61E+07	1.38	0.0729
10	0	1.955E+07	0.91	0.127
0	5	6.47E+06	0.95	0.357
0	7	4.35E+06	1.11	0.621
0	10	5.97E+05	1.22	0.497
6	5	5.97E+07	0.75	0.306

**At ambient temperature*

Overall, epoxy groups on reactive rubber particles give higher crosslink density and consequently enhance the mechanical properties as shown in flexural test. Therefore, 5 wt% RRNP gave higher cross link density than neat epoxy and consequently toughness increased. Incorporating more RRNP percentages lead to some agglomeration and resulting in decreased crosslink density (**Figure 10**). On the other hand, the intercalation and exfoliation of clay platelets in epoxy serve to effectively decrease in crosslink density. That is mean as the number of exfoliated platelets increased as the crosslink density decreased due to molecular mobility. Therefore, sample with 6 wt% of nanoclay containing higher amount of exfoliated platelets as described by XRD and TEM; so it has the lowest crosslink density. The well dispersed nanoclay in epoxy becomes more effective in retarding matrix molecular mobility, thus increasing the storage moduli. It can be seen that the storage modulus increases with increasing clay content up to 6 wt% at rubbery region. Further increase in clay loading

decreases the modulus. The improvement in modulus can be directly ascribed to the stiffening effect of clay fillers since the clay has a higher modulus than epoxy.

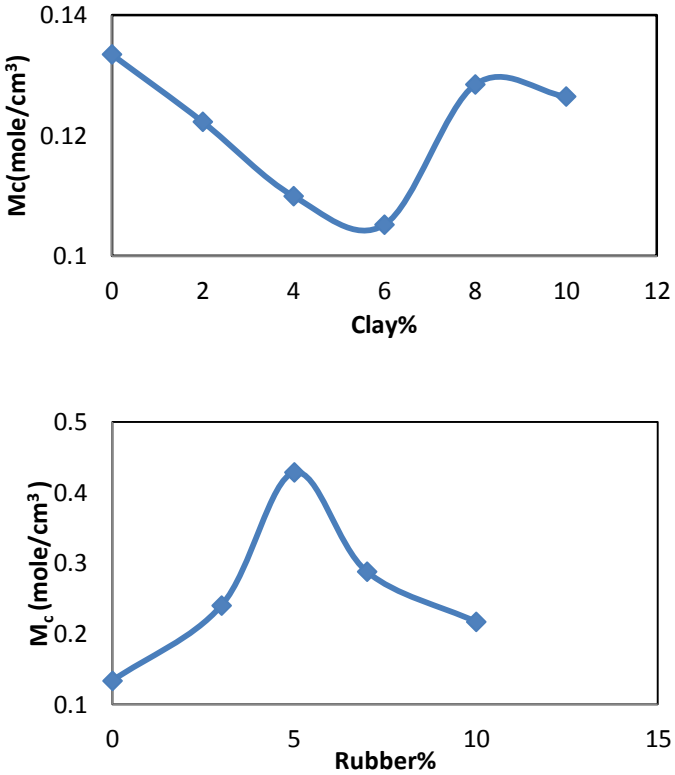

Figure10: Relationship between crosslink density (Mc) and nano-filler percentage: (a) clay/epoxy, (b) RRNP/epoxy nanocomposites

4. CONCLUSIONS

In this work, epoxy/clay/RRNP nanocomposites have been successfully prepared by *in situ* polymerization. Mechanical testing, X-ray diffraction (XRD), Fourier transform infrared spectroscopy (FTIR) and transmission electron microscopy (TEM) were used to measure mechanical, microstructure and morphological properties of the hybrid nanocomposites. Hybrid composites containing (o-mmt) or (RRNP) or both comprise intercalated nanoclay embedded in a homogeneous epoxy matrix. Incorporation of RRNP results in a softened nanocomposite with lower stiffness and improved toughness compared to those of the neat resin. In contrast, incorporation of (o-mmt) in the cured epoxy increased the stiffness and lowered the toughness of the epoxy/nanocomposites compared to those of the neat resin. The morphology of the nanocomposites consists of both exfoliated and intercalated clay structures as evidenced by X-ray diffraction (XRD) and transmission electron microscopy (TEM). The present study is an extended work to characterize the mechanical properties of epoxy and its organoclay nanocomposites, including storage modulus curve by using dynamic mechanical analyzer technique (DMA) and the observed changes are rationalized in the three points bending flexural test data.

5. ACKNOWLEDGMENT

This work was funded by Science and Technology Development Fund (STDF) for US–Egypt (STDF/NSF) Program; Award #3713 and (STDF–CSE) program (ID5213) to Polymer Nanocomposites Center, EPRI, Cairo, Egypt. The authors acknowledge this funding. The

authors also greatly acknowledge funding by the US National Science Foundation (NSF) Award #1103601 through US–Egypt Cooperative Research Program.

REFERENCES

[1] Pham, H. Q.; Marks, M. J. In Kirk-Othmer Encyclopedia of Chemical Technology; Seidel, A.; Ed.; John Wiley & Sons, Inc.: Hoboken, NJ; Vol. **10**, 5th Edition, pp347 -471, 2005.
[2] Sultan, J. N.; McGarry, F. J. Polym. Eng. Sci., **13**, 29−34, 1973.
[3] Yee, A. F.; Pearson, R. A. J. Mater.Sci., **21**, 2475−2488, 1986.
[4] Pearson, R. A.; Yee, A. F. J. Mater.Sci., **26**, 3828−3844, 1991.
[5] Garg, A. C.; Mai, Y.-W.Compos.Sci. Technol., **31**, 179−223, 1988.
[6] Wise, C. W.; Cook, W. D.; Goodwin, A. A. Polymer, **41**, 4625−4633, 2000.
[7] Drake, R. Polym. Mater.Sci. Eng., **63**, 802 -805, 1990.
[8] Pascault, J.-P.Macromol.Symp., **93**, 43 -51, 1995.
[9] Bucknall, C. B. Toughened Plastics; Applied Science Publ.: London, 1977.
[10] Pearson, R. A.; Yee, A. F. J. Mater.Sci., **21**, 2475 -2488, 1986.
[11] Kojima, Y.; Usuki, A.; Kawasumi, M.; Okada, A.; Fukushima, Y.; Kurauchi, T.; Kamigaito, O. J. Mater. Res., **8**, 1185 -1189, 1993.
[12] Yano, K.; Usuki, A.; Okada, A. J. Polym. Sci., Part A: Polym. Chem., **35**, 2289 2294, 1997.
[13] Gilman, J. W.; Kashiwagi, T.; Lichtenhan, J. D. *SAMPE J.*, **33**, 40- 46, 1997.
[14] Vaia, R. A.; Price, G.; Ruth, P. N.; Nguyen, H. T.; Lichtenhan, J. D. Appl. Clay Sci., **15**,67 -92, 1999.
[15] Kandil, U.F., "Novel Functional Ethylene/Propylene Elastomers: Synthesis and Characterization"; Materials Science and Engineering, College of Earth and Mineral Science, Penn State University; PA, USA, 2005.
[16] F. H. Rajabi , M. M. Alavi Nikje and T. Taslimipour; "Epoxidation of Styrene–Butadiene Rubber (SBR) Using In Situ Generated Dimethyldioxirane (DMD): Characterization and Kinetic Study"; Designed Monomers and Polymers **13**, 535–546, 2010.